Supplementary Materials

Clinical Pharmacology and Safety of Parenteral Non-Opioid Analgesics After Cardiothoracic Surgery: An Exploratory Study Integrating Molecular Docking and Network-Based Analysis

Overview

In Silico Molecular Docking Study of Selected NSAIDs and Antipyrine Metabolites Against Key Inflammatory and Cardiovascular Targets: Detailed Methodology and Supplementary Data.

S1. Scope and Purpose of This Supplementary Document

This document provides the complete methodological detail, computational parameter specifications, and ancillary data supporting the molecular docking analyses reported in the main manuscript. All findings presented herein and, in the parent, text are exploratory and hypothesis-generating in character; they represent computational structural observations and should not be interpreted as direct evidence of biological or pharmacological activity. The primary purpose of this supplementary record is to ensure methodological transparency and analytical reproducibility.

S2. Software, Computational Tools, and Version Information

All computational analyses were conducted using the software packages listed in Supplementary Table S1. Version numbers are specified to facilitate reproducibility.

Supplementary Table S1. Software and computational tools employed in the present study

Software/tool	Version	Function	Reference/source
AutoDock	4.2.6	Molecular docking (LGA)	[34]
AutoDockTools (MGLTools)	1.5.6	Receptor/ligand preparation, grid generation	[35]
ChemDraw ultra	12.0	2D ligand structure construction	PerkinElmer Informatics
ChemBio3D ultra	13.0	3D conformation generation, MMFF94 energy minimisation	PerkinElmer Informatics
Open Babel	3.1.1	File format conversion (PDB → PDBQT)	[36]
BIOVIA Discovery studio Visualizer	2025 Client	Interaction analysis and visualisation	Dassault Systèmes BIOVIA
Cytoscape	3.10.4	PPI network visualisation and MCL clustering	[27]

S3. Ligand Preparation

Two-dimensional chemical structures of the seven query ligands — tenoxicam, metamizole, ketoprofen, etofenamate, diclofenac, 4-methylaminoantipyrine (4-MAA), and 4-aminoantipyrine (4-AA) — were constructed in ChemDraw Ultra 12.0. Three-dimensional conformations were generated in ChemBio3D Ultra 13.0 and subjected to energy minimisation using the Merck Molecular Force Field (MMFF94), with convergence to the lowest-energy conformer confirmed prior to export in PDB format.

Ligand files were subsequently converted to PDBQT format using Open Babel (v3.1.1). During preparation, Gasteiger partial charges were assigned to all non-hydrogen atoms, rotatable bonds were identified and parameterised automatically, and polar hydrogen atoms were added explicitly. Conformational flexibility was defined within the

AutoDock parameter framework; the number of active torsional degrees of freedom was optimised for each ligand to balance conformational sampling breadth with computational tractability, ensuring consistency of binding pose comparisons across the compound series.

S4. Receptor Preparation

Crystal structures for all six target proteins were retrieved from the RCSB Protein Data Bank (https://www.rcsb.org). Receptor preparation was performed uniformly in AutoDockTools (MGLTools v1.5.6) according to the following sequential steps: (i) removal of all crystallographic water molecules; (ii) deletion of co-crystallised ligands and heteroatoms not required for active site definition; (iii) addition of polar hydrogen atoms; (iv) assignment of Kollman united-atom partial charges; and (v) export to PDBQT format.

For COX-1 (PDB: 5WBE) and COX-2 (PDB: 5IKR), grid boxes were positioned to encompass the cyclooxygenase channel, incorporating the established Arg120-Tyr355 anchoring region and the adjacent hydrophobic subsites. For NOS3 (PDB: 5UO8), the grid was centred on the haem-proximal active site, encompassing the substrate-binding tunnel. For ACE (PDB: 9SSA), the grid was placed to include the zinc-coordinating histidine triad (His353, His383, His387, His513) and the surrounding S1/S2 subsites. For AGTR1 (PDB: 4ZUD), the orthosteric transmembrane binding cavity was targeted. For IL-6Rα (PDB: 1P9M), the deposited structure represents the hexameric IL-6/IL-6Rα/gp130 signalling complex; accordingly, docking was conducted using an interface-directed approach, with the grid positioned at the IL-6/IL-6Rα protein-protein interaction surface, reflecting exploratory interest in interface modulation rather than canonical enzymatic inhibition.

S5. Docking Protocol

Molecular docking simulations were performed using AutoDock 4.2.6 with the lamarckian genetic algorithm (LGA). For each ligand-protein pair, twenty independent docking runs were executed to ensure adequate conformational sampling. Grid maps were calculated using AutoGrid (part of the MGLTools suite) with a spacing of 0.375 Å. The resulting conformational ensembles were clustered at an RMSD tolerance of ≤2.0 Å; the lowest binding free energy pose within the most populated cluster was selected as the representative binding mode for each complex. Estimated binding free energies (ΔG, kcal/mol) and RMSD values from the reference pose are reported for all complexes in Table 1 of the main manuscript.

S6. Grid Box Coordinates and Dimensions

Supplementary Table S2 provides the precise grid centre coordinates and box dimensions applied for each target protein. Centre coordinates are expressed in Ångström units relative to the crystallographic frame of reference.

Supplementary Table S2. Docking grid parameters for each target protein

Target protein	PDB ID	Grid centre (x, y, z)/Å	Grid dimensions/Å	Grid spacing/Å
COX-1	5WBE	x=36.806, y=163.583, z=27.944	40×40×40	0.375
COX-2	5IKR	x=38.139, y=2.639, z=61.472	40×40×40	0.375
NOS3	5UO8	x=62.028, y=29.472, z=-183.694	40×40×40	0.375
ACE	9SSA	x=-14.611, y=7.444, z=-23.111	40×40×40	0.375
IL-6Rα	1P9M	x=-45.639, y=166.889, z=46.361	40×40×40	0.375
AGTR1	4ZUD	x=-41.000, y=63.250, z=28.750	40×40×40	0.375

S7. Interaction Analysis

Protein-ligand complexes obtained from docking were imported into BIOVIA Discovery Studio Visualizer (2025 Client) for residue-level non-covalent interaction analysis. The following interaction categories were catalogued: conventional hydrogen bonds, π-π stacking interactions (both face-to-face and edge-to-face geometries), π-alkyl and alkyl-alkyl contacts, π-sulfur interactions, and general hydrophobic contacts. Two-dimensional interaction diagrams

and three-dimensional visualisations were generated to illustrate ligand binding orientation and stabilisation patterns within each active site, as presented in Figures 2 and 3 of the main manuscript. It is acknowledged that interaction classification thresholds in BIOVIA Discovery Studio are algorithmically defined and may differ from those of alternative visualisation platforms; consequently, reported interactions should be regarded as indicative rather than definitive.

Supplementary Table S3. Estimated binding free energies (ΔG, kcal/mol), RMSD values, and residue-level non-covalent interaction profiles for all ligand-protein pairs derived from molecular docking simulations. Interactions were analysed using BIOVIA Discovery Studio Visualizer (2025 Client). 4-MAA: 4-methylaminoantipyrine; 4-AA: 4-aminoantipyrine. (-) denotes absence of the respective interaction type.

Compound	ΔG (kcal/mol)	RMSD (Å)	H-bond residues	π-π interactions	Alkyl/π-alkyl	π-sulfur	Target	PDB ID
Tenoxicam	-11.23	0.04	Ser530, Ala527	–	Leu359, Val116, Leu531, Val349	Met522	COX-1	5WBE
Metamizole	-10.52	0.50	Arg120, Ala527	Trp387, Gly526	Leu384, Leu352, Val349	Met522	COX-1	5WBE
Ketoprofen	-9.27	0.62	Arg120, Tyr355	-	Ile523, Val349, Leu359	Met522	COX-1	5WBE
Etofenamate	-9.92	1.26	Arg120, Ser530, Tyr355, His90, Ile523	Phe518, Gly526	Leu352	Met522	COX-1	5WBE
Diclofenac	-9.86	0.24	Tyr348	Trp387	Phe518, Leu352, Leu531	Met522	COX-1	5WBE
4-MAA	-8.31	0.81	Met522	-	Tyr385, Leu531	-	COX-1	5WBE
4-AA	-8.21	0.11	Met522	-	Leu531, Tyr385, Leu384, Trp387, Phe381	-	COX-1	5WBE
Tenoxicam	-11.71	0.42	Tyr385, Ser530, Val523	Phe518, Gly526	Leu531, Leu359, Val349, Val116, Ala527	Met522, Trp387, Phe381	COX-2	5IKR
Metamizole	-9.86	0.71	Arg120, Ser530	-	-	Met522	COX-2	5IKR
Ketoprofen	-9.45	0.20	Arg120, Tyr355, Ser530	-	Ala527, Leu352, Leu359, Leu531,	-	COX-2	5IKR

					Val349, Val116			
Etofenamate	-8.66	0.00	Arg120, Tyr355	-	Ala527, Leu352, Trp387, Leu384, Tyr385	-	COX-2	5IKR
Diclofenac	-9.25	0.93	Ser530, Tyr385	-	Leu352, Val523, Leu531, Val349	-	COX-2	5IKR
4-MAA	-8.73	0.27	Met522	-	Leu352, Val523, Ala527	-	COX-2	5IKR
4-AA	-8.65	0.14	Met522	-	Leu352, Val523, Phe518	-	COX-2	5IKR
Tenoxicam	-9.97	0.22	Cys184	-	-	Phe473	NOS3	5UO8
Metamizole	-9.62	0.18	Gly355, Phe353	-	Cys184, Arg183	Phe353	NOS3	5UO8
Ketoprofen	-9.31	0.35	Phe353, Gly355, Pro334	Trp178	Leu193, Cys184, Val336	-	NOS3	5UO8
Etofenamate	-9.06	1.05	Gly355, Arg183	Phe353, Trp178	Ala181, Cys184	-	NOS3	5UO8
Diclofenac	-9.78	0.25	Pro334, Val336, Cys184	Trp178	Phe473	-	NOS3	5UO8
4-MAA	-8.01	0.07	Val336	Phe353	Pro334	-	NOS3	5UO8
4-AA	-7.54	0.08	Val336	Phe353	Pro334	-	NOS3	5UO8
Tenoxicam	-10.86	0.53	Glu384, His353, His513	-	Val380	-	ACE	9SSA
Metamizole	-8.70	0.90	His353, His513	Phe527	Val379	His513	ACE	9SSA
Ketoprofen	-8.92	0.91	His353, His513, Tyr520	His383, His387	Tyr523, Phe527, Phe457	-	ACE	9SSA
Etofenamate	-7.58	1.64	His353	Tyr523, His383	Val379, Val380	-	ACE	9SSA
Diclofenac	-8.17	0.72	Lys511, Gln281	Tyr523	His383, Val380, Phe527	-	ACE	9SSA
4-MAA	-7.40	0.12	His513	Phe457, His383	His387	-	ACE	9SSA
4-AA	-6.92	0.16	His513, Tyr523	Phe457, His383	His383, His387	-	ACE	9SSA
Tenoxicam	-8.74	0.21	Lys27, Arg30, Arg233	–	Leu254	-	IL-6R	1P9M

Metamizole	-7.89	0.64	Arg30, Arg233, Glu278	–	Leu254	-	IL-6R	1P9M
Ketoprofen	-7.65	0.21	Arg233, Phe234, Val251, Lys252, Asp253	–	Leu254	-	IL-6R	1P9M
Etofenamate	-6.58	1.02	Arg233, Glu278	Phe279	Leu254	-	IL-6R	1P9M
Diclofenac	-7.82	0.26	Arg233, Asp253, Val251, Phe234, Lys252	–	Met250, Ile232	-	IL-6R	1P9M
4-MAA	-7.01	0.11	Arg30	-	Ile232, Val230	-	IL-6R	1P9M
4-AA	-6.74	0.11	Arg30	-	Ile232, Val230	-	IL-6R	1P9M
Tenoxicam	-9.99	0.13	Tyr35	Trp84	Leu81, Cys289	Tyr87	AGTR1	4ZUD
Metamizole	-9.54	0.44	Tyr35, Tyr92	Tyr292	Ile288	Tyr92	AGTR1	4ZUD
Ketoprofen	-8.06	0.57	Arg167, Cys180	Trp84	Val108	-	AGTR1	4ZUD
Etofenamate	-8.51	0.00	Cys180, Tyr92	Tyr87, Trp84, Tyr292	Val108, Ile288	-	AGTR1	4ZUD
Diclofenac	-7.69	0.15	Arg167, Cys180	Trp84	Val108, Tyr35	-	AGTR1	4ZUD
4-MAA	-7.21	0.04	Tyr35	Tyr292	Ile288, Trp84	-	AGTR1	4ZUD
4-AA	-7.56	0.04	Thr88	Trp84	Val108, Pro285, Ile288, Tyr92	-	AGTR1	4ZUD
ACE: Angiotensin-converting enzyme; NOS3: Nitric oxide synthase; IL-6R: Interleukin-6 receptor alpha; COX-1: Cyclooxygenase-1								

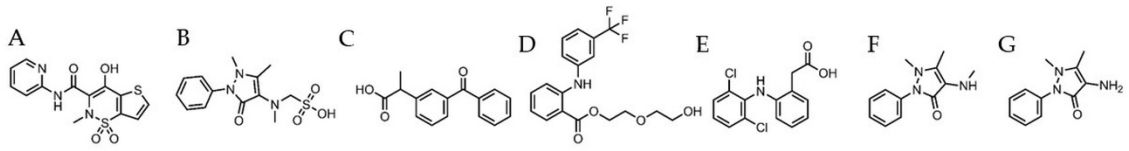

Figure S1. Chemical structures of the compounds included in the docking analysis: **(A)** tenoxicam, **(B)** metamizole, **(C)** ketoprofen, **(D)** etofenamate, **(E)** diclofenac, **(F)** 4-methylaminoantipyrine (4-MAA), and **(G)** 4-aminoantipyrine (4-AA).

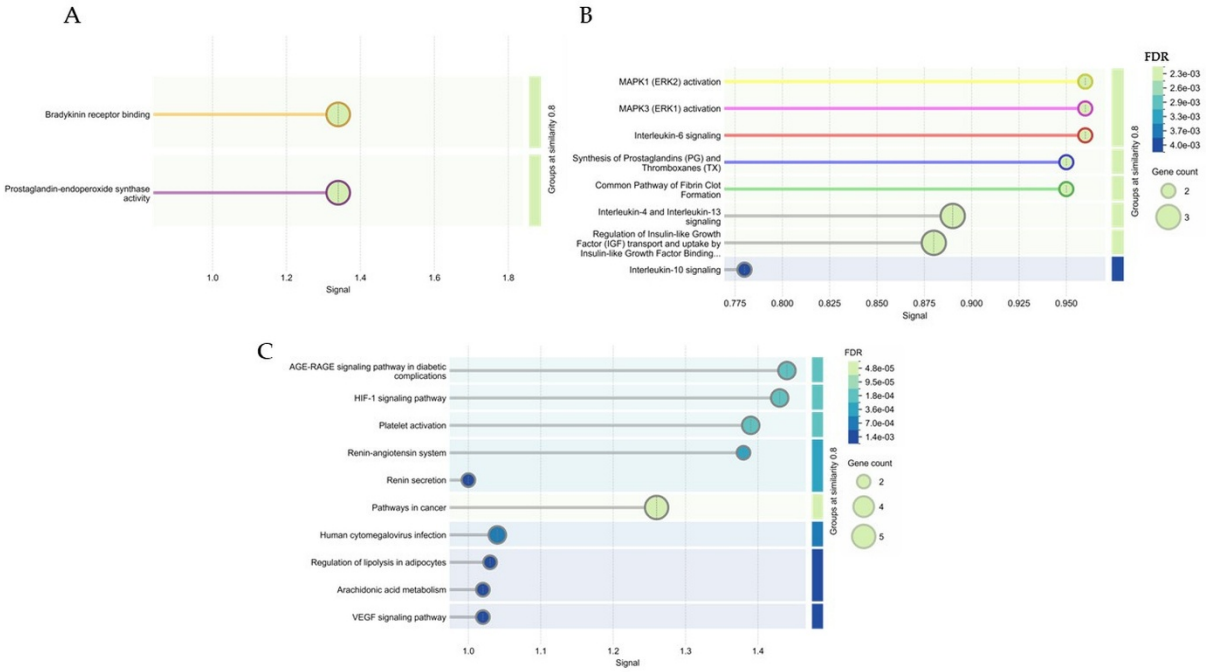

Figure S2. STRING-based enrichment analyses. Extended functional enrichment analyses of the docking-derived interaction network. (A) GO molecular function enrichment analysis, illustrating enzymatic activities and binding functions associated with the network. (B) Reactome pathway enrichment analysis, highlighting signaling pathways related to inflammatory response, coagulation, and intracellular signaling cascades. (C) KEGG pathway enrichment analysis, demonstrating involvement in key biological pathways including vascular regulation, platelet activation, and arachidonic acid metabolism. Bubble size indicates gene count, and color scale represents FDR-adjusted significance values.